Journal of
Nanoscience and Nanotechnology
Vol. 11, 1342–1345, 2011

Disordered Antireflective Subwavelength Structures Using Ag Nanoparticles for GaN-Based Optical Device Applications

Eun Sil Choi[1], Young Min Song[2], Gyeong Cheol Park[2], and Yong Tak Lee[1, 2, 3, *]

[1] *School of Photon Science and Technology, Gwangju Institute of Science and Technology, 1 Oryong-dong, Buk-gu, Gwangju 500-712, Republic of Korea*
[2] *Department of Information and Communications, Gwangju Institute of Science and Technology, 1 Oryong-dong, Buk-gu, Gwangju 500-712, Republic of Korea*
[3] *Department of Nanobio Materials and Electronics, Gwangju Institute of Science and Technology, 1 Oryong-dong, Buk-gu, Gwangju 500-712, Republic of Korea*

This study reports disordered antireflective subwavelength structures (SWS) on GaN and indium tin oxide (ITO) surfaces fabricated using thermally dewetted Ag nanoparticles. It is shown that the average diameter of Ag nanoparticles, which determines the optical characteristics, can be simply controlled by changing the thickness of the Ag thin film and the annealing temperature. The fabricated GaN and ITO SWS with tapered profile exhibited very low reflectance compared to that of a flat surface over a wide wavelength range.

Keywords: Nanoparticles, Gallium Nitride, Indium Tin Oxide, Subwavelength Structures.

RESEARCH ARTICLE

1. INTRODUCTION

GaN-based materials have been widely exploited as active materials for light-emitting diodes (LEDs), laser diodes, and even solar cells due to their tunable energy band gaps, covering almost the entire solar spectrum.[1–5] In most optoelectronic device applications, undesirable reflection between different media degrades the optical efficiency. Thin film coatings with intermediate or graded refractive indices are commonly used to suppress the undesired Fresnel reflection. However, stability problems induced by adhesiveness and thermal mismatch are often associated with such approaches.[6–7]

Recently, subwavelength structures (SWS) have attracted considerable interest in optoelectronic device applications due to their broadband and omnidirectional antireflection properties as well as their good thermal stability and durability.[8–12] For the fabrication of SWS, the masks are commonly formed by e-beam[6] or laser interference lithography,[10] which increases the production time and cost. In this study, disordered GaN SWS on GaN/Sapphire substrates were fabricated using thermally dewetted Ag nanoparticles to reduce the surface reflection. Because indium tin oxide (ITO) is usually used to GaN-based devices as a current spreading layer, ITO SWS on ITO/GaN/Sapphire substrates were also fabricated. The optical characteristics of each fabricated structure were analyzed by reflectance measurements.

2. EXPERIMENTAL DETAILS

The schematic diagram of the fabrication procedure used in this study is illustrated in Figure 1. A silicon-doped *n*-GaN layer with a thickness of 5-μm was grown on a *c*-plane sapphire (0001) substrate by metal organic chemical vapor deposition (MOCVD). For the fabrication of GaN SWS, 50 nm-thick SiO_2 layer was deposited on GaN/Sapphire substrates using plasma enhanced chemical vapor deposition (PECVD). Then, Ag thin film with a thickness of 20 nm was deposited. Subsequently, a thermal dewetting process was carried out at 500 °C for 1 min under nitrogen flowing gas of 15 sccm to form Ag nanoparticles as etch masks. The SiO_2 layers were patterned by reactive ion etcher (RIE) in a CF_4/O_2 gas mixture. To form the GaN SWS with a tapered profile, the underlying GaN layer was etched using Ag/SiO_2 nanomasks in ICP-RIE under $SiCl_4$/Ar (7.5 sccm/30 sccm) at RF power of 150 W for 5 min. To remove the residual

*Author to whom correspondence should be addressed.

 1533-4880/2011/11/1342/004 doi:10.1166/jnn.2011.3378

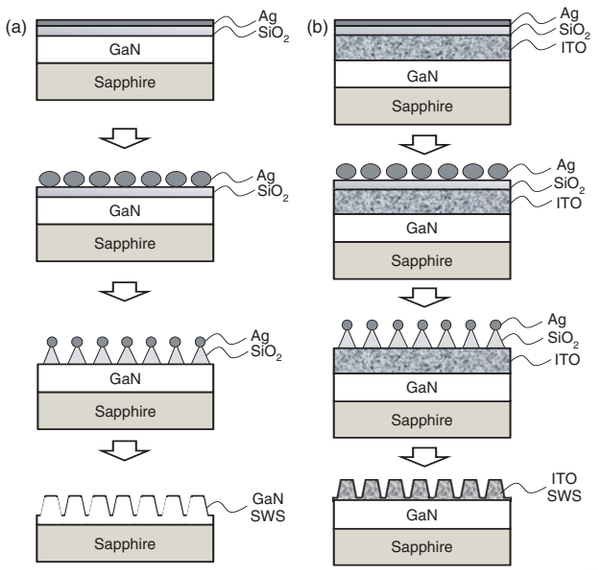

Fig. 1. Schematic diagram of the overall process of (a) fabrication of GaN SWS on GaN/Sapphire and (b) fabrication of ITO SWS on ITO/GaN/Sapphire by thermal dewetting and dry etching processes.

Ag/SiO_2, the samples were dipped into a heated nitric acid (HNO_3) at 80 °C for 10 min and a buffered oxide etcher (BOE) for 10 min, respectively.

For the fabrication of ITO SWS, ITO film with a thickness of 400 nm was deposited on GaN/Sapphire substrates using an e-beam evaporator. It was then annealed at 500 °C for 1 min under an air atmosphere. The following fabrication processes were essentially identical to those of the GaN SWS except for the ITO etching and the removal process of the residual Ag/SiO_2. A gas mixture of $CH_4/H_2/Ar$ (20/40/20 sccm) was used to form the ITO SWS. The residual Ag/SiO_2 was removed by RIE in a CF_4/O_2 gas mixture.

3. RESULTS AND DISCUSSION

Two-dimensional metal films deposited on dielectric substrates are typically thermo-dynamically unstable and, when heated, become rough as a result of dewetting.[9] Figure 2 shows the SEM images of the Ag thin films on SiO_2/GaN/Sapphire (a) as-deposited with a thickness of 30 nm and annealed at 500 °C for 1 min under a nitrogen atmosphere with thicknesses of (b) 5 nm, (c) 10 nm, (d) 20 nm, and (e) 30 nm. Because the surface energy of Ag film is much higher than that of SiO_2 film, Ag film is unstable on SiO_2, resulting in the dewetting of the film with the annealing process. To clarify the characteristics of the Ag nanoparticles, the diameter distributions of the Ag nanoparticles were estimated using a commercial image processor. As shown in Figure 2(f), the average diameter is increased as the deposited film thickness increases, which are analogous to a previous study in which an

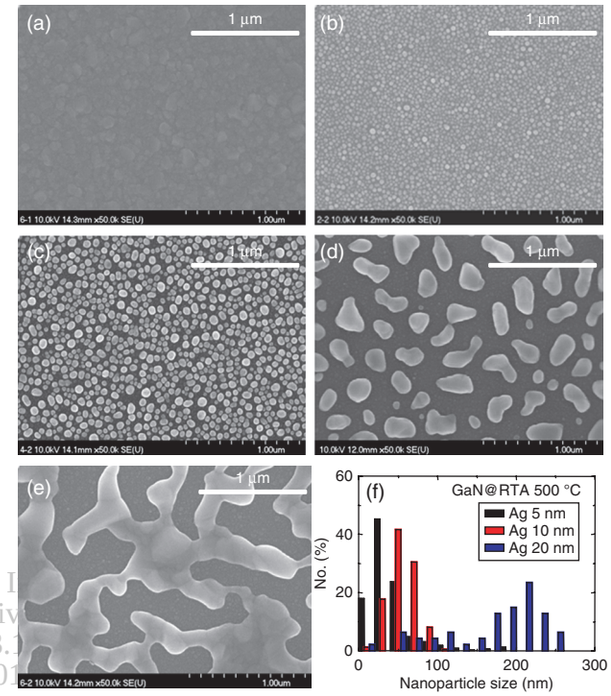

Fig. 2. SEM images of the Ag thin films on SiO_2/GaN/Sapphire (a) as-deposited (30 nm) and annealed at 500 °C for 1 min with thicknesses of (b) 5 nm, (c) 10 nm, (d) 20 nm, and (e) 30 nm. (f) Diameter distribution of Ag nanoparticles with different deposited film thickness.

e-beam induced dewetting process was used. Thick Ag films (>30 nm) lead to large and bicontinuous shapes, that are not adequate for subwavelength mask patterns.

Figure 3 shows images of 20 nm-thick Ag films on SiO_2/GaN/Sapphire for annealed samples at temperatures of (a) 400 °C, (b) 500 °C, (c) 600 °C, and (d) 700 °C for 1 min. As a higher annealing temperature enhances the surface energy of thin film, the Ag thin film is completely

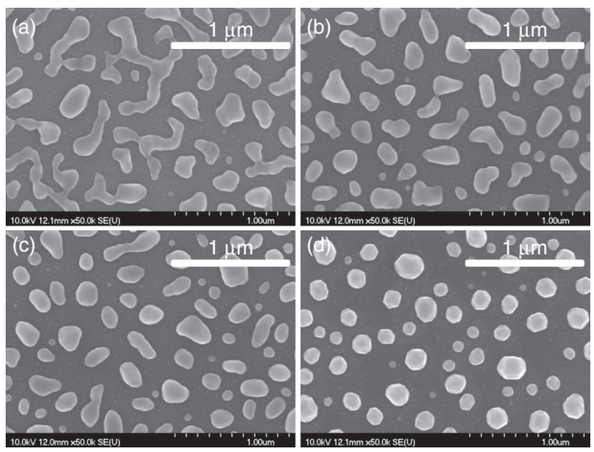

Fig. 3. SEM images of surface morphologies of Ag (20 nm) on SiO_2/GaN/Sapphire for annealed samples at temperatures of (a) 400 °C, (b) 500 °C, (c) 600 °C, and (d) 700 ° for 1 min.

RESEARCH ARTICLE

agglomerated into a hemispherical nanodot array of a subwavelength scale as the heating time increases. In practical applications, however, the annealing temperature and time should be carefully chosen considering the damage from unwanted heating.

The reflectance of the fabricated SWS at normal incidence was measured using a spectrophotometer (Cary 5000, Varian). Figure 4 shows the measured reflectance as a function of the wavelength for fabricated GaN SWS on GaN/Sapphire substrates with different etching times. As shown in Figure 4, after 1 min etching, there was no significant reflectance difference compared to that on a flat surface. However, the reflectance of SWS etched for more than 5 min was found to be less than 5% over a wide wavelength range of 300–800 nm. A longer etching time (i.e., 9 min etching) leads to lower reflectance, because the effective refractive index is changed more gradually in case of the SWS with a taller height.[9] At this point of view, nanotip arrays with a tip height up to 1 μm are ideal for broadband antireflection. However, it is evident that a taller height generally requires complex process steps in optoelectronic device applications.

The effect of gas mixture determines the proportion of the chemical and physical reaction during the etching process, which affects the sidewall profile of the etched structure. Figure 5 shows the measured reflectance of the fabricated GaN SWS with different $SiCl_4$/Ar gas mixtures. As shown in the inset of Figure 5, additional Ar gases enhance the physical reaction, which causes the shape of the etched pattern to be more abrupt, especially at 30 sccm. In order to obtain lower reflectance over a wide wavelength range, the SWS should have conical or pyramidal shape, which induce the graded effect refractive index. In other words, the SWS with non-tapered sidewall such as nanorod cannot guarantee the broadband antireflection.

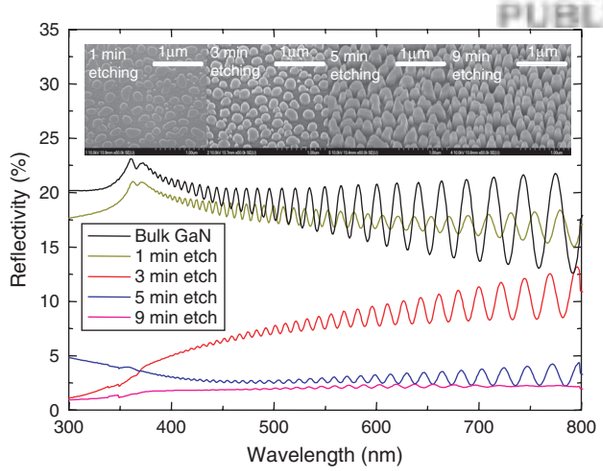

Fig. 4. Measured reflectance of the fabricated GaN SWS on GaN/Sapphire corresponding to the etching times of 1, 3, 5, and 9 min. The inset show the SEM images of the fabricated GaN SWS with different etching times.

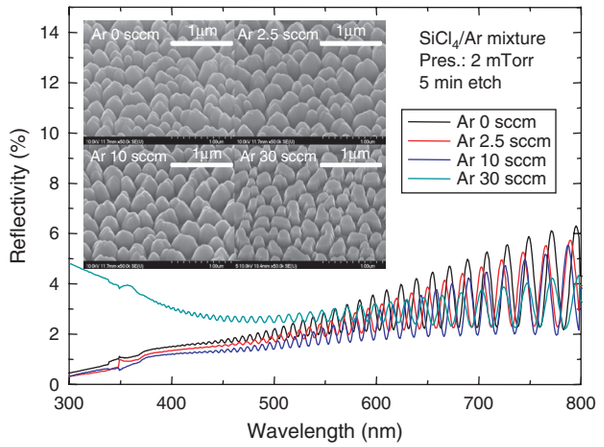

Fig. 5. Measured reflectance spectra of the fabricated GaN SWS on GaN/Sapphire with Ar gas flow rate of (a) 0 sccm, (b) 2.5 sccm, (c) 10 sccm, and (d) 30 sccm. The inset show the SEM images of the fabricated GaN SWS structures with different Ar gas flow rate.

That's why the GaN SWS fabricated at Ar 30 sccm has higher reflectance at shorter wavelength ranges.

In the SWS fabrication, the insertion of a SiO_2 layer plays two major roles. It serves as both a durable etch mask and a buffer layer to form Ag nanoparticles. If the surface material is changed, the dewetting time and temperature should be modified due to surface tension between two materials. However, this difficulty can be

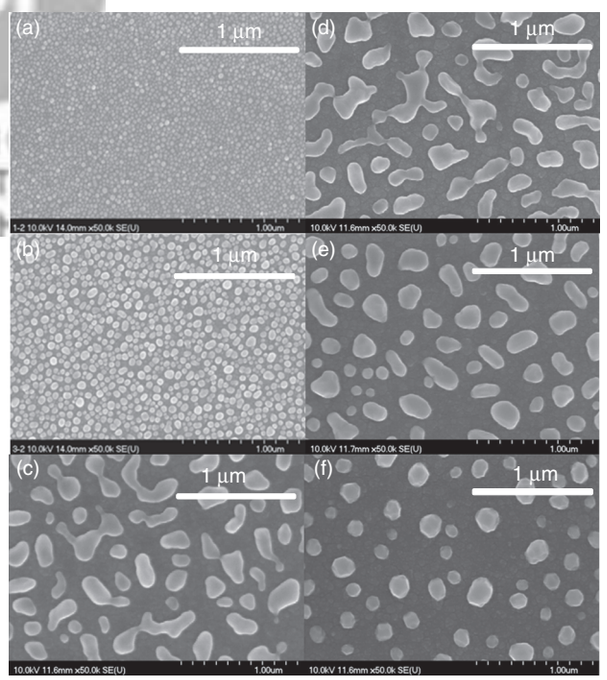

Fig. 6. SEM images of the Ag thin film on SiO_2/ITO/GaN/Sapphire annealed at 500 °C for 1 min with thicknesses of (a) 5 nm, (b) 10 nm, and (c) 20 nm. (d)∼(f) 20 nm-thick Ag thin film annealed at (d) 400 °C, (e) 600 °C, and (f) 700 °C.

RESEARCH ARTICLE

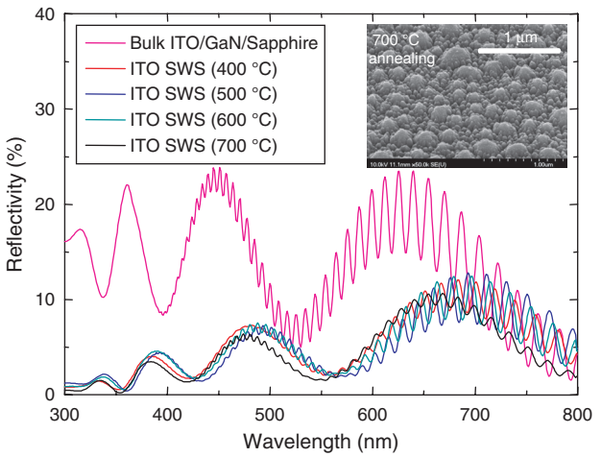

Fig. 7. Measured reflectance of the fabricated ITO SWS on ITO/GaN/Sapphire as a function of wavelength with annealing temperatures of 400 °C, 500 °C, 600 °C, and 700 °C. Inset shows the SEM image of the fabricated ITO SWS annealed at temperature of 700 °C.

easily solved by inserting a SiO_2 layer. Figure 6 shows SEM images of Ag thin film on SiO_2/ITO/GaN/Sapphire substrates with various film thicknesses and annealing temperatures. As expected, there were no remarkable changes compared to when Ag nanoparticles were deposited on SiO_2/GaN/Sapphire substrates due to the insertion of a SiO_2 layer.

Figure 7 shows the measured reflectance of the ITO SWS on ITO/GaN/Sapphire substrates. All curves have fluctuations due to the multiple interferences of light at each interface. While the ITO flat surface shows reflection maxima of ∼23%, the fabricated ITO SWS shows the reflection maxima of ∼12%, which depends somewhat on the annealing temperature. Even though the ripple pattern cannot be removed completely due to the multiple interferences, the ITO SWS shows 61% reduced mean reflectance in a wavelength range of 300 to 800 nm.

4. CONCLUSION

To reduce the surface reflection of GaN and ITO, SWS of GaN and ITO were fabricated by thermally dewetted Ag nanoparticles. The effects of the film thickness, annealing temperature, etching time and gas mixture on the reflection properties were then investigated. The surface reflection of the GaN and ITO decreased substantially due to the optimized SWS over a wide wavelength range. From these results, these SWS are believed to be cost-effective and suitable for high-efficiency GaN-based optical devices.

Acknowledgment: This work was partially supported by the IT R&D program of MKE/IITA [2007-F-045-03] and by the Core Technology Development Program for Next-generation Solar Cells of Research Institute for Solar and Sustainable Energies (RISE) at GIST.

References and Notes

1. S. Nakamura and G. Fasol, The Blue Laser Diode, Springer, New York (**1997**).
2. M. Koike, N. Shibata, H. Kato, and Y. Takahashi, *IEEE J. Sel. Topics Quantum Electron* 8, 271 (**2002**).
3. H. Morkoc, S. Strite, G. B. Gao, M. E. Lin, B. Sverdlov, and M. Burns, *J. Appl. Phys.* 76, 1363 (**1994**).
4. S. J. Pearton, B. S. Kang, B. P. Gila, D. P. Norton, O. Kryliouk, F. Ren, Y.-W. Heo, C.-Y. Chang, G.-C. Chi, W.-M. Wang, and L.-C. Chen, *J. Nanosci. Nanotechnol.* 8, 99 (**2008**).
5. F. Leonard Deepak, A. Govindaraj, and C. N. R. Rao, *J. Nanosci. Nanotechnol.* 1, 303 (**2001**).
6. P. Lalanne and G. M. Morris, *Nanotechnology* 8, 53 (**1997**).
7. Y. Kanamori, M. Sasaki, and K. Hane, *Opt. Lett.* 24, 1422 (**1999**).
8. H. Kikuta, H. Toyota, and W. J. Yu, *Opt. Rev.* 10, 63 (**2003**).
9. Y. M. Song, S. Y. Bae, J. S. Yu, and Y. T. Lee, *Opt. Lett.* 34, 1702 (**2009**).
10. Y. C. Chang, G. H. Mei, T. W. Chang, T. J. Wang, D. Z. Lin, and C. K. Lee, *Nanotechnology* 18, 285 (**2007**).
11. Y. M. Song, E. S. Choi, J. S. Yu, and Y. T. Lee, *Opt. Exp.* 17, 20991 (**2009**).
12. Y. M. Song, J. S. Yu, and Y. T. Lee, *Opt. Lett.* 35, 276 (**2010**).

Received: 14 November 2009. Accepted: 26 March 2010.

RESEARCH ARTICLE